Thermo-Mechanical Properties of Poly -Caprolactone/Poly L-Lactic Acid Blends: Addition of Nalidixic Acid and Polyethylene Glycol Additives Journal of the Mechanical Behavior of Biomedical Materials

Douglas, P., Albadarin, A., Al-Muhtaseb, A. H., Mangwandi, C., & Walker, G. (2015). Thermo-Mechanical Properties of Poly -Caprolactone/Poly L-Lactic Acid Blends: Addition of Nalidixic Acid and Polyethylene Glycol Additives Journal of the Mechanical Behavior of Biomedical Materials. Journal of the Mechanical Behavior of Biomedical Materials, 45, 154-165. DOI: 10.1016/j.jmbbm.2015.01.022

Published in:
Journal of the Mechanical Behavior of Biomedical Materials

Document Version:
Peer reviewed version

Thermo-Mechanical Properties of Poly ε-Caprolactone/Poly L-Lactic Acid Blends: Addition of Nalidixic Acid and Polyethylene Glycol Additives

P. Douglas[1], Ahmad B. Albadarin[1,2*], Ala'a H. Al-Muhtaseb[3],

Chirangano Mangwandi[1] and G.M. Walker[1,2]

[1]School of Chemistry and Chemical Engineering, Queen's University Belfast, Belfast BT9 5AG, Northern Ireland, UK.
[2]Materials Surface Science Institute, Department of Chemical and Environmental Sciences, University of Limerick, Ireland
[3]Petroleum and Chemical Engineering Department, Faculty of Engineering, Sultan Qaboos University, Muscat-Oman.

*Corresponding Author: Dr Ahmad B. Albadarin

Email: Ahmad.B.Albadarin@ul.ie

Department of Chemical and Environmental Sciences, University of Limerick.

Tel: +44 74 6080 5982; fax: +44 28 9097 6524.

Abstract:

The search for ideal biomaterials is still on-going for tissue regeneration. In this study, blends of Poly ε-caprolactone (PCL) with Poly l-lactic acid (PLLA), Nalidixic Acid (NA) and Polyethylene glycol (PEG) were prepared. Mechanical and thermal properties of the blends were investigated by tensile and flexural analysis, DSC, TGA, WXRD, MFI, BET, SEM and hot stage optical microscopy. Results showed that the loading of PLLA caused a significant decrease in tensile strength and almost total eradication of the elongation at break of PCL matrix, especially after PEG and NA addition. Increased stiffness was also noted with additional NA, PEG and PLLA, resulting in an increase in the flexural modulus of the blends. Isothermal degradation indicated that bulk PCL, PLLA and the blends were thermally stable at 200°C for the duration of 2h making extrusion of the blends at this temperature viable. Morphological study showed that increasing the PLLA content and addition of the very low viscosity PEG and powder NA decreased the Melt Flow Indexer and increased the viscosity. At the higher temperature the PLLA begins to soften and eventually melts allowing for increased flow and, coupling this with, the natural increase in MFI caused by temperature is enhanced further. The PEG and NA addition increased dramatically the pore volume which is important for cell growth and flow transport of nutrients and metabolic waste.

Keywords: Poly ε-Caprolactone; Poly L-lactic Acid; Polyethylene Glycol; Mechanical Properties; Thermal Properties; Topography.

1. INTRODUCTION

Poly ε-caprolactone (PCL) is a biodegradable linear aliphatic polyester with low melting point (55–65°C) and glass transition temperature (60°C) (Woodruff & Hutmacher, 2010). It is produced by chemical synthesis from crude oil via the ring opening polymerization of caprolactone monomer and it possesses high toughness but relatively low strength, and thus has a rubber-like nature (Chu, 2003). PCL is one of the many biodegradable polymers widely used in medicine and pharmacology as drug carriers because it is a biocompatible and undergoes natural biodegradation in the human body while not releasing any harmful compounds. PCL was also suggested for use in the production of common-use articles and packaging materials, including packaging intended for food which significantly hinders environmental pollution from poly(ε-caprolactone) waste (Moraczewski, 2014). However, the rather high crystallinity of PCL decreases its compatibility with soft tissues and lowers its biodegradability. These drawbacks may obstruct its application in drug-controlled release systems (Zhou et al., 2003). Blending two polymers is an approach to develop new biomaterials exhibiting combinations of properties that could not be obtained by individual polymers (Sarasam & Madihally, 2005). Blending PCL with other materials has proven to be an effective method to enhance the biodegradability of the resulting composites (Fernández et al., 2013; Little et al., 2009; Tuba et al., 2011; Valdés García et al., 2014). Zhou and co-workers synthesized Poly(ε-caprolactone)-poly(ethylene glycol) (PECL) copolymers using stannous octoate as catalyst at 160°C by bulk polymerization (Zhou et al., 2003). All PECL copolymers formed microspheres containing human serum albumin (HSA) which can be used as drug delivery carriers in medical applications. Fernández and co-workers studied the effect of chain microstructures on mechanical behavior and aging of a poly(L-lactide-co-ε-caprolactone) biomedical thermoplastic-elastomer (Fernández et al., 2012). The PLCL showing a random character closest to the Bernoullian distribution of sequences ($l_{LA} = 1/CL$) was found to exhibit higher strain capability and strain recovery values and is less prone to

supramolecular arrangements. Physical aging leads also to dramatic changes in tensile behavior of the moderately blocky PLCLs that evolved from being an elastomeric to be partly a glassy semicrystalline thermoplastic, and, thus, can eventually condition its potential uses for medical devices. The in vitro release of proteins from novel, biodegradable phase-separated poly(ε-caprolactone-PEG)-block-poly(ε-caprolactone), [PCL-PEG]-b-[PCL]) multiblock copolymers was studied by (Stanković et al., 2014). It was found that the release rate of the protein increased with decreasing molecular weight of the protein and with increasing PEG content of the polymer. The swelling and degradation rate of the copolymer increased with increasing PEG content. Blends of PLA and PCL have been prepared using a block copolymer of poly(ethylene glycol) and poly(propylene glycol) as a compatibilizer to enhance phase miscibility (Chavalitpanya & Phattanarudee, 2013). Also, pore hydrophilic polymers and forming additives are added to the formulation to increase the release rate by improving the porosity of the pellet during dissolution (Douglas et al., 2010). The effect of an active agent and pore former on the mechanical, thermal and rheological properties of polycaprolactone is an area in which very little has been published in literature. Therefore, this work mainly investigate the effect of the copolymer PLLA on both the bulk PCL matrix and the bioactive PCL and PEG blends. Moreover, the study investigates how the processing methods of these blends affect post extrusion the nalidixic acid release characteristics. The main aims of this work were to evaluate the mechanical, thermal and topographical modifications of the prepared blends.

2. MATERIALS AND METHODS

2.1 Materials

All materials used in this study, Poly (ε–caprolactone) (PCL) (Solvay Caprolactones with grade number 6500); Poly l-lactic acid (PLLA) (Sigma–Aldrich); Nalidixic Acid (NA) (Tyresk Chemicals with a 98% purity) and Polyethylene glycol (PEG) (Sigma–Aldrich) along with their physical properties are presented in details in a previous study by Douglas and co-workers (Douglas et al., 2010). Also, samples preparation procedures including extrusion and pressing has been described in the same previous study. In brief, materials were blended into their particular compositions in a high speed mixer at 1800 ± 5rpm for 5min (Rondol DAC150, UK). Then, the mixtures were fed into a 25mm Twin Screw Extruder at 120 ± 1 rpm and 80–90 ± 2 °C (Dr Collin Z25, Germany), to produce a continuous strand of each blend using a gravimetric feeder. The strand was quenched in a water bath, at a temperature of 20 ± 0.5 °C, and then passed through a pelletiser. Please check our previous work for the experimental design and materials compositions used (Douglas et al., 2010). In the analysis and testing part, all tests were performed in triplicate unless indicated.

2.2 Analysis and Testing

2.3.1 Tensile and Flexural Analysis

All tensile tests were performed with a load cell of 5 kN at a constant crosshead speed of 50 mm/min using an Instron Universal Tensile Tester 4411. For each blend, at least five replicates were tested. As the samples were pressed from isotropic platens into dumbbell strips with a length of 80 mm and a thickness of 1 mm, no difference in mechanical properties was expected with testing direction and was confirmed by the similarity of the Young's Modulus results for PCL, i.e. 373 ±40 and 380 ±35 MPa in the machine and transverse direction, respectively. For the flexural tests, the three point compression bending tests were performed using a 5 kN load cell and a support span of 25 mm with sample dimensions of 50

× 10 × 1.5 mm. Three specimens were tested per group. All flexural tests were carried out in accordance with ASTM D790M using an Instron Universal Tensile Tester 4411.

When the test pieces are deflected, a continuous graduation of stress occurs from a maximum tensile stress on one surface through a neutral axis to a maximum compressive stress on the other surface.

2.3.2 Dynamic Mechanical Thermal Analysis

All samples were scanned using a Polymer Labs Mark II DMTA at a frequency of 1 Hz over the temperature range of –120 to 40°C at a scan rate of 2°C/min with the exception of the virgin PLLA sample which was scanned over the range of 0 to 120°C. The cut-off point of 20°C was chosen due to the melting of PCL occurring over the range of 45°C to 65°C. This phase transition would have overshadowed the glass transition of the PLLA (occurring at ~55°C) in the samples containing blends of PCL and PLLA. A low frequency was chosen since, provided the strains are also low, heat build-up is negligible (Brown, 1999); at larger frequencies and strains, a larger heat build-up can occur. Cooling to –120°C was obtained by using a cryogenic chamber within the machine.

2.3.3 Differential Scanning Calorimetry

All DSC analyses were undertaken in both a Perkin Elmer DSC 6 and a Perkin Elmer Diamond DSC (Perkin Elmer, USA). For each test, between 5 and 7 mg of sample was cut from the plaques, weighed and then sealed in an aluminium sample pan. When using the DSC 6, all samples were subjected to a heating rate of 2°C/min from 20 to 250°C to determine the melting temperature and percentage crystallinity of the sample. The effect of processing history was removed by heating, cooling at 2°C/min and then reheating to 250°C at the same rate. When using the Diamond DSC, all samples were subjected to a heating rate of 100°C/min from –100 to 100°C to determine any changes in the glass transition temperature of the sample. Again the effect of processing history was removed by heating, cooling and

reheating the sample at the same rate (100°C/min). The percentage crystallinity of the sample was determined using the first melting endotherm by calculating the area under the resultant curve between the points of inflexion around the melting peak and dividing this by a reference value.

2.3.4 Thermogravimetric Analysis

Thermogravimetric Analysis (TGA) using TA Instruments TGA Q500, USA was carried out. Weighed samples of each of the blends were placed into the TGA machine and ramped from 15 to 500°C at 10°C/min. Additional samples were ramped from 15 to 200°C at 10°C/min and then held under isothermal conditions at 200°C for 120 min in order to determine the thermal stability of the blends under sustained excess temperatures.

2.3.5 Thermal Conductivity

Thermal Conductivity (*k*) (Armfield HT10XC, UK) is an intensive property of a sample indicating its ability to conduct heat in semi-static surroundings. *k* depends on the structure and temperature of the sample, and can be greatly affected by the degree of crystallinity of a sample as different conductivities occur along different crystal axis. Low density polymers exhibit *k* values usually in the range 0.16 to 0.33 $Wm^{-1}K^{-1}$ at room temperature (Cremers & Fine, 1991). All *k* measurements were made using a service unit at 50% applied voltage and 25% water flow. The conductivities recorded were simple steady state conduction in one dimension and are considered to be comparative only. Samples were pressed into 50 x 50 x 1mm plaques for analysis.

2.3.6 Wide Angle X-Ray Diffraction (WXRD)

WXRD (PANalytical X'Pert Pro, UK) was used to determine the crystallographic properties of the blends by observing the scattering intensity of an X-ray hitting the sample as a function of incident and scattering angle. The wavelength used was that for measuring diamond at 1.5418367 Å. The average crystallite size (or size broadening) was determined using the

Debye-Scherrer formula. The orientation of the crystals was determined using Hermans Orientation function while the Broadening due to strain (ε_{str}) in the material was then calculated using the formula presented in (Wilson, 1949).

2.3.7 Melt Flow Index (MFI)

A Melt Flow Indexer (Kayeness Galaxy Model 7024, UK) was employed as a single capillary rheometer for the investigation of the flow properties of the blends. The rheological characteristics of the blends were determined by measuring the mass flow rate of the melt under the loading condition of 2.16 kg at temperatures of 90, 125, 160 and 200°C.

2.3.8 Hot Stage Optical and Scanning Electron Microscopy

Sample preparation included microtoming the specimens to 1000 × 2500 × 5 μm dimensions, sealed between 2 glass slips and placed into the hot stage platform of the microscope (Nikon Eclipse ME600, Germany) attached with a temperature control unit (Linkam Instrumentals D600, UK) and Liquid Nitrogen Pump with magnifications of ×20 and ×50 lens and ×10 eyepiece (overall magnifications ×200 and ×500). The specimens were heated from 30 to 250°C at 10°C/min and held at this temperature for 4 min to eliminate processing history. The specimens were then cooled at 5°C/min to 0°C and digital images were taken every 0.1s in order to capture the onset and end temperatures of crystallisation and calculation of the rate of crystal growth (Schulze & Biermann, 1993). Scanning Electron Microscopy (SEM) was used to study the blends at magnifications of ×1000 and ×15000. All samples were coated with gold atoms using a sputter coater under vacuum and argon gas. Once conductive, the samples were then placed into the High Vacuum Microscope (JEOL JSM-6490, Japan) under vacuum and analysed at 0.5 kV accelerating voltage for variations in surface quality before and after drug release.

3 RESULTS AND DISCUSSIONS

3.1 Mechanical Properties

3.1.1 Tensile Properties

The tensile properties of the PCL-PLLA blends are shown in Table 1. The loading of the PLLA into the PCL matrix at the largest concentration of 25% (w/w) had a detrimental effect on the tensile strength and the elongation at break. The results shown in Figure 1A indicate that the addition of 5% (w/w) PLLA reduced the tensile strength and elongation at break by 32% and 85% respectively. This concentration level was chosen as it was in accordance with that used in the literature (commonly 20% (w/w)) (Maglio et al., 2003; Semba et al., 2006). At the low loading of the PLLA, there were significant changes in the tensile properties which continued with increasing loading of PLLA and with the addition of the PEG and NA, as can be seen in Figure 1a. From these data, it can be assumed that PLLA content, even at low levels, is one of the main causes of decreasing elongation in the PCL matrix. Also apparent is the recovery of the "elongation at break" with the addition of PEG, which lubricates the PCL chains allowing increased stretching.

Figure 1B illustrates the effect of PLLA on the stiffness of the blends. Overall, the addition of PLLA appears to reinforce the blends, increasing the Young's Modulus. This is apparent at both the 5% and 25% (w/w) PLLA. However at the high loading of 25% (w/w) PLLA, although still higher than that of pure PCL, the Young's Modulus has decreased. It is therefore assumed that an overall immiscible blend is formed between the PCL and the PLLA. The Young's Modulus increased by 40% for the lowest loading of PLLA, but then decreased with increased loading and upon addition of PEG and NA, as shown in Figure 1B. These results are directly comparable with those found by Hijanen-Vainio and co-worker who determined the properties of several copolymerised blends of PCL-PLLA. For a 25% w/w PLLA blend in PCL they found stress at break values of 19 MPa and an elongation at break value of ~ 7% (Hiljanen-Vainio et al., 1996). However it was found that, while physical

blending i.e. extrusion, is a credible approach to altering the properties of the PCL with PLLA, this method tended to neglect the specific interaction between the homopolymer and its minor components. Therefore, Hijanen-Vainio's results obtained from reactive blending would be considered a more accurate description of the processes taking place.

3.1.2 Flexural Properties

The flexural modulus of the PCL-PLLA blends is illustrated in Figure 1C. It can be seen that the addition of the PLLA has a notable effect on the flexural modulus of the PCL matrix. The increase in stiffness is attributed to increase in PLLA (% wt), which is an extremely brittle polymer that is known to impart increased stiffness in blends. On the inclusion of the PEG into the 5% (w/w) PLLA blend, the degree of stiffness decreases to that of the pure PCL. However the increased flexibility is counterbalanced by the loading of NA into the 5% PLLA-5% PEG (w/w), which again imparts stiffness as the free volume within the PCL is reduced further. When comparing the value for the modulus of 5% PLLA with that of 5% NA and 5% PEG (data not shown here), it was found that the PLLA produces the smallest increase in stiffness, with recorded values of 413±59 MPa for the 5% PLLA, 485±46 MPa for the 5% NA and 468±39 MPa for the 5% PEG. Similar values of flexural modulus were found in non-conventional injection-moulded blends of PLLA and PCL (470 MPa) (Altpeter et al., 2004).

3.1.3 Dynamic Mechanical Thermal Analysis

The mechanical transitions of the blends are shown in Table 2 and Figure 2. Again the β and α transitions are observed, but it is clear that the addition of the PLLA to the PCL has a significant damping effect on the β transition so that it is almost eradicated thus limiting side chain movement. Again, the data indicate that the shear modulus decreases as the testing temperature increases and reduces sharply at the glass transition where there is a corresponding large peak in tan δ. The small change in the peak α transition and also in the Tg can be considered negligible and therefore confirms immiscibility between the polymers, as a

large shift would be expected in the Tg of the 25% PLLA blend closer to that of the PLLA, measured at 60°C. The dampening effect on the tan δ peak caused by the addition of PLLA in PCL making it more crystalline and the subsequent shift in the Tg has been reported (Lostocco & Huang, 1997). Again, the stiffening effect of both the PLLA and the NA is revealed by the increasing storage modulus values recorded at ambient conditions.

3.2 Thermal Properties

3.2.1 Differential Scanning Calorimetry

Non-isothermal DSC: using scan rates of both 2°C/min and 100°C/min, the non-isothermal crystallisation of the blends was investigated. The thermogram of pure PLLA is shown in Figure 3A. Detectable are the glass transition at approximately 62°C, the recrystallisation exotherm of the PLLA (since it was crash cooled during processing and therefore considered completely amorphous), the melting endotherm at 180°C with a calculated 33.2% crystallinity and the cooling exotherm occurring at 101°C. The thermal stability becomes compromised at temperatures in excess of 220°C with the increase in energy being attributed to degradation. Table 3 details the changes in melt temperature, degree of crystallinity, melt profile and crystallisation temperature associated with the PLLA in the PCL matrix. As observed at a scan rate of 2°C/min, increasing PLLA content has little effect on the melting and cooling temperatures of the PCL, as shown in Figure 3B. Also, crystal reorganisation during the melting process remains unchanged due to the slow scan rate, which allows for melt separation of varying crystal size i.e. smaller crystals melt first as they require a lower enthalpy of fusion than larger crystals. The melting width however decreases with PLLA in all blends, thereby making the crystal size distribution narrower. This also indicates that the crystals will be of more uniform size.

The degree of crystallinity in the blend formulations increases with the addition of PLLA but this effect decreases with increased loading. This could be due to the “nucleating effect” that the PLLA copolymer has on the PCL i.e. the solid regions of PLLA act as sites for crystal

growth. The increased crystallinity is confirmed by the dampening of the tan δ reported in section (3.1.3). The increased loading causes a decrease in the crystallinity, as larger concentrations of PLLA begin to impede crystal growth. Figure 3B shows the melting behaviour of the PCL-PLLA blends and that of pure PLLA. The melting point of 180°C is clearly visible, indicating that PLLA is in the solid state during the melting and crystallisation of PCL. The Tg of the pure PLLA, which is clearly visible at 59°C, is reduced to approximately 52°C when incorporated into the blends. Generally, it is difficult to determine exactly the transition temperatures of the blends as peaks overlap and in some samples peak broadening occurs. However two trends were apparent from this analysis: the Tg of the PLLA is essentially unchanged from that of the pure PLLA, and the Tm of PCL is also unchanged. These findings were also reported by Broz and co-workers (Broz et al., 2003) who using a 20% PLLA fraction in PCL, found the Tg of PLLA to be ~53°C and the Tm of PCL as 63°C. Also, the re-crystallisation and crystallisation which normally occurs in amorphous PLLA at 100°C and 180°C is not visible in the lower weight fraction blends due to the low concentration. In a study carried out by (Lostocco & Huang, 1997), the PLLA phase did not exhibit the ability to crystallise when incorporated into PCL and this was attributed to the occurrence of ester reactions between the two polymers limiting the average sequence length of the PLLA. This limited chain length was below the critical length required for chain folding. The data indicate that, during cooling, the peak cooling temperature decreased with increasing cooling rate (see Tables 3 and 4). This decrease in crystallisation temperature is caused by the inability of the PCL chains to maintain the cooling rate. The non-isothermal melting data presented in Table 4 for a heating rate of 100°C/min show little variation in cooling temperature. However, the melting peak gradually decreases with increased PLLA content and additive loading, leading to significant variation in the enthalpy of fusion. This may be explained by the rapid scan rate used, which imparts thermal lag into the system. As with the NA, the PLLA appears to have a depressive effect on the melt temperature that

causes the formation of less thermodynamically stable crystals within the blends. These less stable crystals require less energy to melt thus lowering the melt temperature. The wide variability of the 100°C/min rate is shown in Figure 4.

Isothermal Crystallisation: the isothermal crystallisation of the PCL-PLLA blends was studied at 38°C over a 40 min period. Under these conditions crystal formation is no longer cooling controlled. Figure 5A and Table 5 illustrate the isothermal behaviour of the PCL-PLLA blends. The data indicate that loadings up to 25% (w/w) PLLA decreases the isothermal crystallisation of the PCL, thus implying that the PCL has become more amorphous. The addition of the copolymer caused a decrease in the overall crystallisation time. However, a reduction in the rate of crystallisation for blends containing solely the copolymer was noted. This indicates a greater number of amorphous regions now present in the PCL and an associated increase in molecule hindrance.

3.2.2 Thermogravimetric Analysis

Thermogravimetric analysis (TGA) was undertaken on the blends to a maximum temperature of 500°C, with the decomposition profiles shown in Figure 5B and degradation data in Table 6. The onset of thermal degradation of virgin PCL was determined to be approximately 400°C with this degradation temperature decreasing with increasing NA loading. This also resulted in a more pronounced plateau on the decomposition curve. The thermal decomposition of the PLLA was found in this study to be 350°C which shows good comparison with the value of 331°C reported by (Wu et al., 2006) on their work using PDLA nanocomposites. The negative effect that PLLA has on PCL decomposition is probably due to autocatalysis of PLLA during its decomposition, promoting the early onset of PCL degradation. This decrease in the thermal decomposition temperature is further exacerbated by the incorporation of the PEG and even more so with the NA, which also promotes the early onset of PCL degradation. When the blends were subjected to isothermal TGA at 200°C for 96 min, pure PCL was shown to be

thermally stable, as was PLLA, which showed < 1% weight reduction over the duration of the test as observed in Figure 5C. This isothermal degradation ultimately affects the extruder processing temperature, since long residence times near the onset of thermal degradation should be avoided in order to maintain structural integrity, drug efficacy and device quality. Loading the PCL-PLLA blends with NA saw the blends undergo degradation at 40 min with continual degradation for the duration of the analysis. As discussed, this degradation was attributed solely to the NA.

3.2.3 Thermal Conductivity

The thermal conductivity of the PCL-PLLA blends was measured under ambient conditions. Values of 0.26 and 0.10 W/m°C were determined for the bulk PCL and PLLA respectively. On the addition of the PLLA to the PCL matrix at 5% (w/w) loading, the conductivity decreased considerably to 0.15 W/m°C. Conductivity continued to decrease with further addition of the PLLA to 0.13 W/m°C, indicating a degree of miscibility between the polymers. This partial miscibility is therefore assumed to exist only at the boundary of the copolymers, as the PLLA did not undergo melting during processing, and acted as a large filler throughout these analyses. As the boundary is minuscule in comparison with the volume of the polymers, immiscibility is assumed, which is confirmed by the increased stiffening in the mechanical properties and the unaffected glass transition temperature.

3.2.4 Wide Angle X-ray Diffraction (WXRD)

WXRD analysis was carried out on the PCL-PLLA blends to determine the interaction between the crystal phases of both materials. Analysing Figure 6 confirms the lack of interaction between the phases. The major crystal peaks of pure PCL at 2θ = 21.26, 21.86 and 23.57° are present and un-altered in all blends, with no new peaks being observed as the PLLA was in the amorphous state. On the addition of the PEG, two new peaks are identified at 26.9 and 28.5° and these are attributed to the highly crystalline structure of the PEG. The

new peak at 11.7° in the blend containing all additives is attributed to the crystal structure of the NA. From Table 7, the distance between the crystals in all the blends remains relatively unchanged, corresponding to a value of 4.2 Å regardless of loading. The orientation of the crystals also remained planar with a Hermans orientation function of 1. The average crystallite size was determined from the Debye-Scherrer formula, the results of which are presented in Table 7 and are based on the assumption that there is no strain within the lattice (Rezgui et al., 2005). On the addition of PLLA, a small increase in the average crystallite size (calculated from the Scherrer formula) within the crystals is noted from 113 to 120 Å, as the PLLA acts as a nucleating agent. A further increase in PLLA loading caused the average crystallite size to shift back to 110 Å. No crystallite information and therefore broadening data could be obtained for the PLLA as it was in the amorphous state. The addition of the amorphous PLLA causes a notable decrease in the strain broadening of the crystallites, indicating that lattice imperfections are decreased. These imperfections lead to the displacement of atoms from their sites, causing deviation from the ideal crystal structure and thus microstrain.

3.3 Morphology and Topography

3.3.1. Melt Flow Index

The MFI was used to compare the processing viscosity of the blends at varying temperature with a constant shear rate, as dual capillary rheology data could not be obtained for the PCL-PLLA blends. This was due to the large increase in viscosity caused by even small quantities of addition of the PLLA to the PCL making flow through the 1 mm diameter impossible at 90°C. The temperatures used were 90, 120, 160 and 200°C and samples were tested using ASTM D1238-99, Solvay Caprolactones Ltd. As observed in Table 8, the addition of PLLA at the lower temperatures caused a decrease in the MFI, indicating an increase in the viscosity. Increasing the loading of the PLLA from 5 to 25% (increasing filler content) caused a continual decrease in MFI and increase in viscosity. At the higher temperatures, an increase in

MFI was noted for all of the loadings, which produced a decrease in viscosity and made the melt more Newtonian. At the higher temperature the PLLA begins to soften and eventually melts allowing for increased flow and, coupling this with the addition of the very low viscosity PEG and powder NA, the natural increase in MFI caused by temperature is enhanced further. Figure 7 indicates that the PCL-PLLA blends become more Newtonian with increasing temperature, at all loadings. Moreover, at temperatures of 160 and 200°C this effect continues for loadings up to 25% w/w PLLA.

3.3.2. BET Pore Analysis

The results of PCL-PLLA blends pore size and volume are presented in Table 9. The results indicate that the addition and increasing amounts of the PLLA causes no significant variation in the surface area. However, on addition of the PEG, the surface area more than doubled, due to its low molecular weight. The average pore size calculated at approximately 21 Å for the bulk PCL was shown to remain relatively unchanged with the addition of small quantities of the PLLA, PEG and NA. However, on loadings of 25% (w/w) PLLA, the average pore size increases, resulting in the expected reduction in surface area. Any small pores will have a larger surface area than fewer larger pores. No significant difference was noted in the total pore volume with PLLA addition but, on addition of the pore former and the drug, the pore volume increased dramatically. Again, the applied BET multipoint model was utilised and was found to be successful in describing the surface area ($r^2 > 0.990$).

3.4 Microscopy

3.5.1 Hot Stage Optical Microscopy

Hot stage optical microscopy was carried out to determine the crystal size of the PCL and the PLLA blends. The amorphous state of the PLLA was maintained by rapid cooling of the blends within the stage. Furthermore, the rate of crystal growth was determined for the blends by melting and cooling the blends and measuring crystal radius before impingement. From the

crystal size and growth measurements (data presented in Table 10 and Figure 8A), the small size and high quantity of the PCL crystals is noted. As stated earlier, the amorphous PLLA and small crystal size of the PCL is due to the rapid cooling rate of 100°C/min, which was used to mimic standard industrial processes. All images show that the PCL spherulites completely fill the area of view and that they are composed of lamellae spreading from nuclei. On the addition of a small amount of the PLLA into the PCL matrix, an increase in PCL crystal size is observed, coupled with a decrease in the rate of growth. This would suggest that the PLLA affects the kinetics of PCL crystal growth, thus reducing the time taken before impingement occurs. It should be noted that the rate quoted in Table 10 is that calculated for crystal growth in the transverse direction only. However, the PLLA could cause the PCL to grow initially in the longitudinal direction, thus explaining the decrease in rate. The crystal size distribution becomes narrower with increased loading of PLLA, thus confirming a decrease in melting width as postulated in section (3.2.1). The darker regions present in Figures 8C and 8D are attributed to PLLA and PEG regions within the PCL. Due to the phase separation, it was not possible to determine the crystal size of these materials in the blends using this method. Also, visible in Figure 8D are the fringed or dendrite crystals of the 5% (w/w) NA blend. These dendritic crystals occur due to instabilities in the growth rate caused by rapid cooling or by the addition of fillers into the polymeric matrix. The determination of the size of the crystals is illustrated in Figure 8B. The optical microscope was also able to detect by observation the onset of thermal degradation in the NA due to the colour change from white to pink.

3.5.2 Scanning Electron Microscopy

The smooth surface of the PLLA is visible in Figure 9. This smooth surface is also evident upon the addition of the PLLA to the PCL. However, on addition of the 5% (w/w) PEG (Figure 9) to the PCL-PLLA blends, a large number of surface defects were observed. Figure

9 shows the effect of adding NA to the PCL-PLLA. The surface coverage of individual NA irregular polygons is extensive, each having an approximate length of 5 μm.

CONCLUSIONS

- The loading of PLLA caused a significant decrease in tensile strength and almost total eradication of the elongation at break of PCL matrix. A brittle blend was produced with the addition of high loadings of the PLLA which resulted in an increase in the PCL Young's Modulus.
- Isothermal crystallisation rate increased with the addition of PLLA and caused a decrease in the heat of fusion. Isothermal degradation indicated that bulk PCL, PLLA and the blends were thermally stable at 200°C for the duration of 2 h making extrusion of the blends at this temperature viable. Using WXRD, PLLA was found to be amorphous and therefore no new peaks were identified in the blends; however the relevant WXRD peaks were identified for the addition for the PEG and the NA.
- Both PCL and amorphous PLLA have similar bonding patterns therefore it was difficult to distinguish variations. The addition of the PEG and NA resulted in new bonding patterns.
- No significant difference was noted in the surface area of the blends on addition of PLLA and other additives.
- Rate of crystal growth decreased with PLLA addition, indicating a possible preferential initial crystal growth in the longitudinal direction. Addition of NA to the PCL-PLLA blends caused formation of dendritic crystals.

REFERENCES

Altpeter, H., Bevis, M.J., Grijpma, D.W., Feijen, J. 2004. Non-conventional injection molding of poly(lactide) and poly(ε-caprolactone) intended for orthopedic applications. *Journal of Materials Science: Materials in Medicine*, **15**(2), 175-184.

Brown, R. 1999. Handbook of Polymer Testing. *1st Edition, CRC Press LLC, SPE.*

Broz, M.E., VanderHart, D.L., Washburn, N.R. 2003. Structure and mechanical properties of poly(d,l-lactic acid)/poly(ε-caprolactone) blends. *Biomaterials*, **24**(23), 4181-4190.

Chavalitpanya, K., Phattanarudee, S. 2013. Poly(Lactic Acid)/Polycaprolactone Blends Compatibilized with Block Copolymer. *Energy Procedia*, **34**(0), 542-548.

Chu, C.C. 2003. eds. J.B. Park & J.D. Bronzino, Biodegradable Polymeric Biomaterials: An Updated Overview" in Biomaterials: Principles and Applications. *1st Edition, CRC Press LLC*, 95-115.

Cremers, C.J., Fine, H.A. 1991. Thermal Conductivity 21, 1st Edition. *Springer, London*.

Douglas, P., Andrews, G., Jones, D., Walker, G. 2010. Analysis of in vitro drug dissolution from PCL melt extrusion. *Chemical Engineering Journal*, **164**(2–3), 359-370.

Fernández, J., Etxeberría, A., Sarasua, J.R. 2013. Effects of repeat unit sequence distribution and residual catalyst on thermal degradation of poly(l-lactide/ε-caprolactone) statistical copolymers. *Polymer Degradation and Stability*, **98**(7), 1293-1299.

Fernández, J., Etxeberria, A., Ugartemendia, J.M., Petisco, S., Sarasua, J.-R. 2012. Effects of chain microstructures on mechanical behavior and aging of a poly(L-lactide-co--caprolactone) biomedical thermoplastic-elastomer. *Journal of the Mechanical Behavior of Biomedical Materials*, **12**(0), 29-38.

Hiljanen-Vainio, M., Karjalainen, T., Seppälä, J. 1996. Biodegradable lactone copolymers. I. Characterization and mechanical behavior of ε-caprolactone and lactide copolymers. *Journal of Applied Polymer Science*, **59**(8), 1281-1288.

Little, U., Buchanan, F., Harkin-Jones, E., McCaigue, M., Farrar, D., Dickson, G. 2009. Accelerated degradation behaviour of poly(ε-caprolactone) via melt blending with poly(aspartic acid-co-lactide) (PAL). *Polymer Degradation and Stability*, **94**(2), 213-220.

Lostocco, M., Huang, S. 1997. The Synthesis and Characterization of Polyesters Derived from L-Lactide and Variably-Sized Poly(Caprolactone). in: *Polymer Modification*, (Eds.) G. Swift, C. Carraher, Jr., C. Bowman, Springer US, pp. 45-57.

Maglio, G., Migliozzi, A., Palumbo, R. 2003. Thermal properties of di- and triblock copolymers of poly(l-lactide) with poly(oxyethylene) or poly(ε-caprolactone). *Polymer*, **44**(2), 369-375.

Moraczewski, K. 2014. Characterization of multi-injected poly(ε-caprolactone). *Polymer Testing*, **33**, 116–120.

Rezgui, F., Swistek, M., Hiver, J.M., G'Sell, C., Sadoun, T. 2005. Deformation and damage upon stretching of degradable polymers (PLA and PCL). *Polymer*, **46**(18), 7370-7385.

Sarasam, A., Madihally, S.V. 2005. Characterization of chitosan–polycaprolactone blends for tissue engineering applications. *Biomaterials*, **26**(27), 5500-5508.

Schulze, G.E.W., Biermann, M. 1993. Growth of one spherulite around a rectangular obstacle. *Journal of Materials Science Letters*, **12**(8), 533-536.

Semba, T., Kitagawa, K., Ishiaku, U.S., Hamada, H. 2006. The effect of crosslinking on the mechanical properties of polylactic acid/polycaprolactone blends. *Journal of Applied Polymer Science*, **101**(3), 1816-1825.

Stanković, M., Tomar, J., Hiemstra, C., Steendam, R., Frijlink, H.W., Hinrichs, W.L.J. 2014. Tailored protein release from biodegradable poly(ε-caprolactone-PEG)-b-poly(ε-caprolactone) multiblock-copolymer implants. *European Journal of Pharmaceutics and Biopharmaceutics*, **87**(2), 329-337.

Tuba, F., Oláh, L., Nagy, P. 2011. Characterization of reactively compatibilized poly(d,l-lactide)/poly(ε-caprolactone) biodegradable blends by essential work of fracture method. *Engineering Fracture Mechanics*, **78**(17), 3123-3133.

Valdés García, A., Ramos Santonja, M., Sanahuja, A.B., Selva, M.d.C.G. 2014. Characterization and degradation characteristics of poly(ε-caprolactone)-based composites reinforced with almond skin residues. *Polymer Degradation and Stability*, **108**(0), 269-279.

Wilson, A. 1949. X-ray diffraction by random layers: ideal line profiles and determination of structure amplitudes from observed line profiles. *Acta Crystallographica*, **2**, 245-251.

Woodruff, M.A., Hutmacher, D.W. 2010. The return of a forgotten polymer—Polycaprolactone in the 21st century. *Progress in Polymer Science*, **35**(10), 1217-1256.

Wu, D., Wu, L., Wu, L., Zhang, M. 2006. Rheology and thermal stability of polylactide/clay nanocomposites. *Polymer Degradation and Stability*, **91**(12), 3149-3155.

Zhou, S., Deng, X., Yang, H. 2003. Biodegradable poly(ε-caprolactone)-poly(ethylene glycol) block copolymers: characterization and their use as drug carriers for a controlled delivery system. *Biomaterials*, **24**(20), 3563-3570.

Table 1: Tensile properties of PCL–PLLA blends.

Blend	Stress at Break (MPa)	% Elongation at Break	Young's modulus (MPa)
PCL	32	783	373
5%PLLA	21	120	513
25% PLLA	21	9	454
5%PLLA–5%PEG	18	26	322
5%PLLA–5%PEG–5%NA	13	7	316

Table 2: Transition temperatures and modulus for PCL–PLLA blends.

Blend	***β*** **(°C)**	**Tg (°C)**	**log E'**	**Storage modulus (MPa)**
PCL	–76	–40	8.45	302
5%PLLA	–74	–36	8.50	285
25%PLLA	–74	–37	8.60	445
5%PLLA–5%PEG	–75	–35	8.50	343
5%PLLA–5%PEG–5%NA	–75	–36	8.50	292

Table 3: Melting properties of the PCL–PLLA blends at 2°C/min.

Blend	**T_m (°C)**	**ΔH_m obs (J/g)**	**ΔH_m theor (J/g)**	**Width (°C)**	**T_c(°C)**	**Shape**
PCL	62.4	79.7	79.7	5.8	33.3	Q
5%PLLA	62.6	84.2	88.7	4.6	36.5	R
25%PLLA	62.4	64.1	85.5	5.0	32.9	R
5%PLLA–5%PEG	62.3	83.7	83.0	4.8	34.7	R
5%PLLA–5%PEG–5%NA	62.6	73.4	57.7	4.3	37.3	M

Table 4: Melting properties of the PCL–PLLA blends at 100°C/min.

Blend	**T_m (°C)**	**ΔH_m obs (J/g)**	**ΔH_m theor (J/g)**	**Width (°C)**	**T_c(°C)**	**Shape**
PCL	80.2	70.8	70.8	28.5	22.3	Q
5%PLLA	76.4	77.5	81.6	20.4	25.3	R
25%PLLA	74.4	63.8	85.1	19.4	24.2	R
5%PLLA–5%PEG	77.9	76.9	70.5	29.5	22.7	R
5%PLLA–5%PEG–5%NA	70.3	62.8	47.4	19.1	22.6	R

Table 5: Isothermal analysis for PCL–PLLA blends at 38°C.

Blend	ΔH (J/g)	t (min)	$t_{1/2}$ (min)	Rate (J/g min)
PCL	32.5	1.7	0.9	18.2
5%PLLA	17.0	1.1	0.7	15.1
25%PLLA	15.8	1.3	0.6	11.1
5%PLLA–5%PEG	23.0	1.0	0.5	23.0
5%PLLA–5%PEG–5%NA	22.3	1.1	0.5	21.5

Table 6: Decomposition data for PCL–PLLA blends.

Blend	Decomposition temp (°C) for blend
PCL	398
5%PLLA	395
25%PLLA	365
5%PLLA–5%PEG	386
5%PLLA–5%PEG–5%NA	310
PLLA	350

Table 7: WXRD analysis for PCL–PLLA blends.

Blend	Bragg's spacing (Å)	Hermans orientation	Scherrer size broadening (D_v)	Strain broadening (ε_{str})
PCL	4.18	1	113	0.07
5%PLLA	4.16	1	120	0.02
25%PLLA	4.15	1	110	0.02
5%PLLA–5%PEG	4.15	1	91	0.02
5%PLLA–5%PEG–5%NA	4.15	1	115	0.02
PLLA	5.52	1	–	–

Table 8: Melt Flow Index (MFI) of PCL–PLLA blends.

Blend	MFI (g/10min)			
	90°C	**125°C**	**160°C**	**200°C**
PCL	3.48	8.95	18.20	34.63
5%PLLA	2.98	7.46	15.95	31.17
25%PLLA	1.29	3.69	7.59	19.23
5%PLLA–5%PEG	3.24	9.25	18.45	42.58
5%PLLA–5%PEG–5%NA	3.20	8.72	22.54	42.53

Table 9: Pore analysis for PCL–PLLA blends.

Blend	Ave. pore size (Å)	Total pore volume (cc/g)	Surface area (m^2/g)	r^2
PCL	21.2	0.072	67.8	0.996
5%PLLA	21.3	0.080	75.5	0.991
25%PLLA	25.4	0.063	49.4	0.997
5%PLLA–5%PEG	21.8	0.144	131.3	0.999
5%PLLA–5%PEG–5%NA	21.5	0.138	128.9	0.991
PLLA	21.7	0.195	178.9	0.993

Table 10: Optical microscopy properties of the PCL–PLLA blends.

Blend	Size (µm)	Rate (µm/s)
PCL	5 – 68	14
5%PLLA	8 – 13	6
25%PLLA	7 – 9	3
5%PLLA–5%PEG	3 – 5	1
5%PLLA–5%PEG–5%NA	~3	8

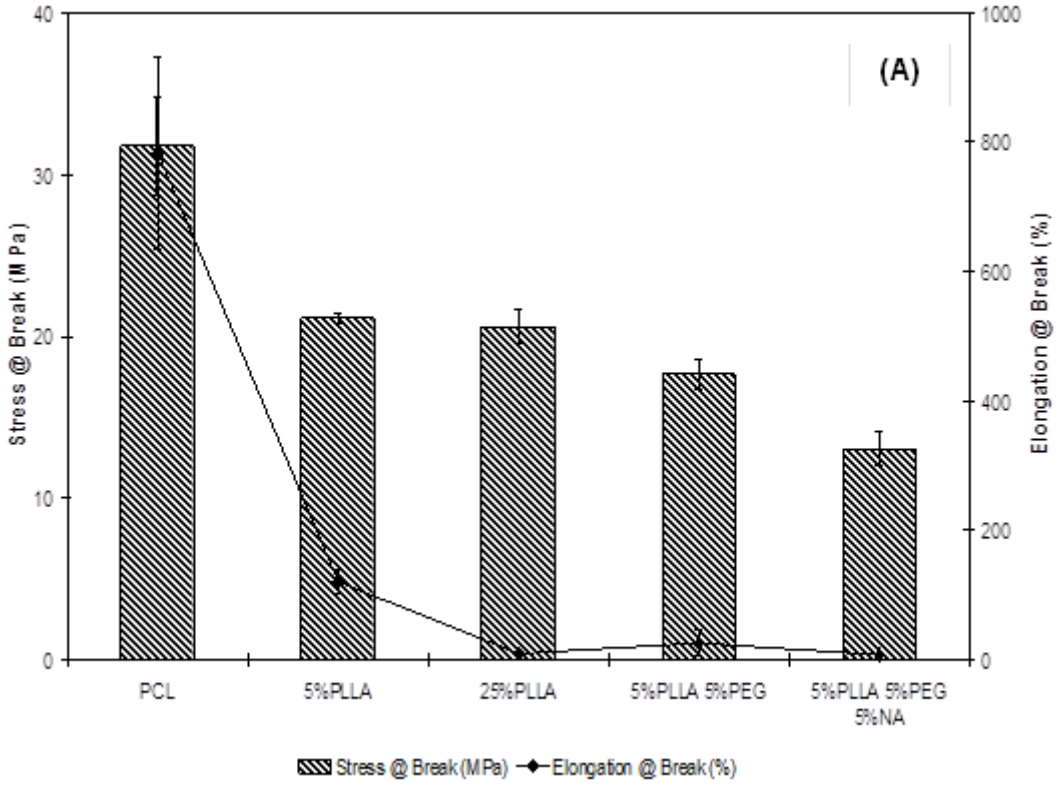
(A)
Stress @ Break (MPa)
Elongation @ Break (%)
40
30
20
10
0
1000
800
600
400
200
0
PCL
5%PLLA
25%PLLA
5%PLLA 5%PEG
5%PLLA 5%PEG 5%NA
Stress @ Break (MPa)
Elongation @ Break (%)

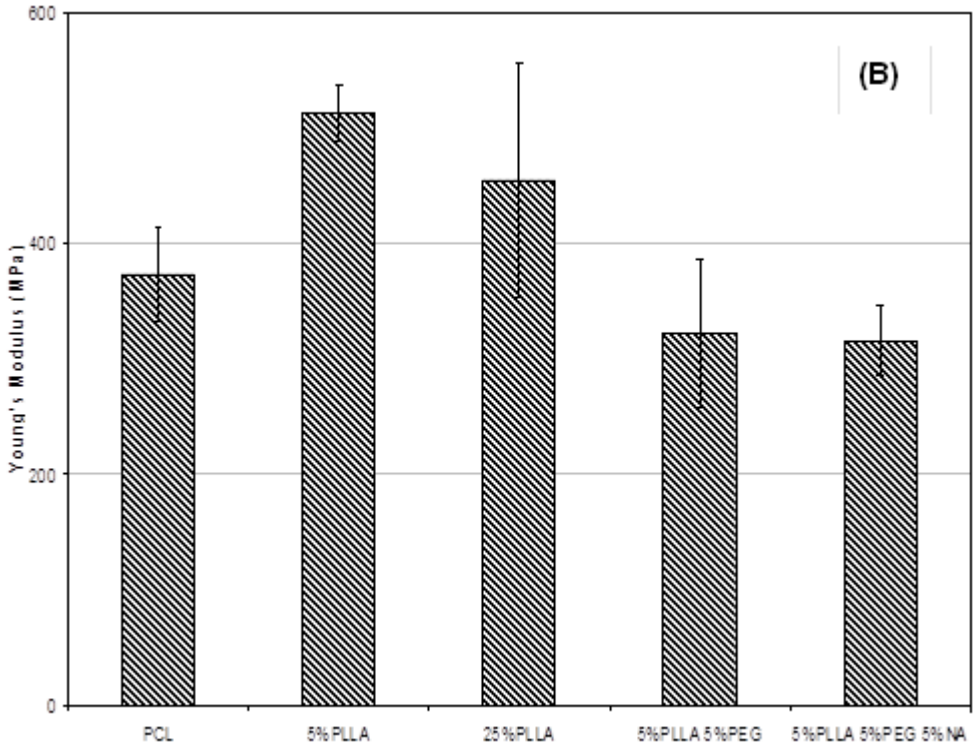
(B)
Young's Modulus (MPa)
600
400
200
0
PCL
5%PLLA
25%PLLA
5%PLLA 5%PEG
5%PLLA 5%PEG 5%NA

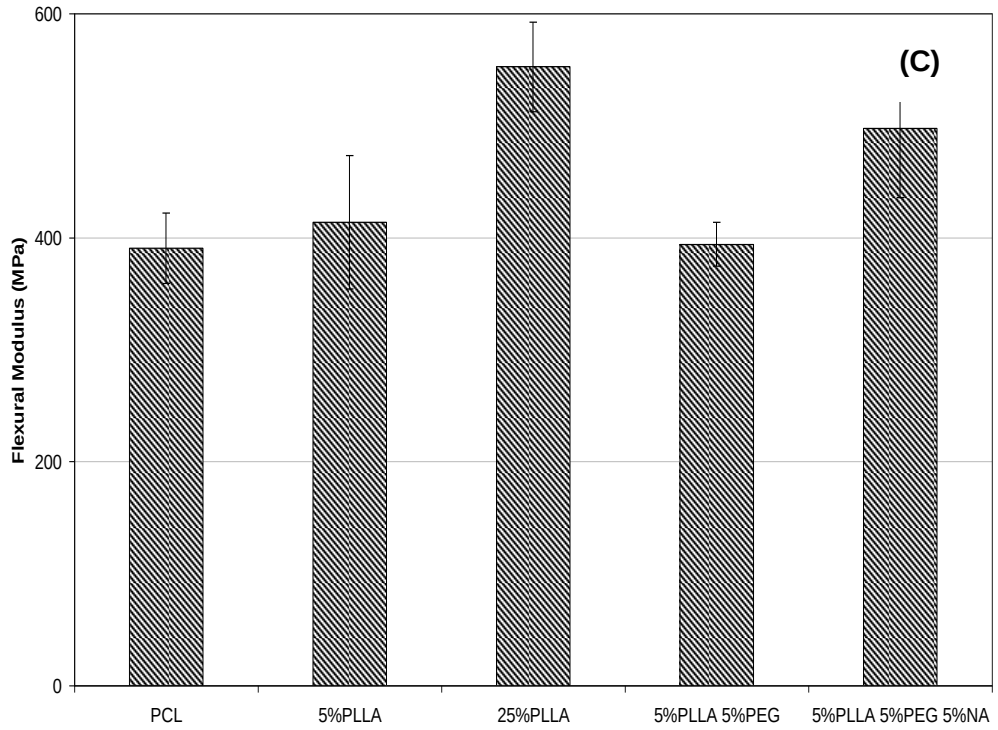

Figure 1: (A) Tensile strength and elongation at break of PCL-PLLA blends; (B) Young's modulus of PCL-PLLA blends; (C) Flexural modulus of PCL-PLLA blends.

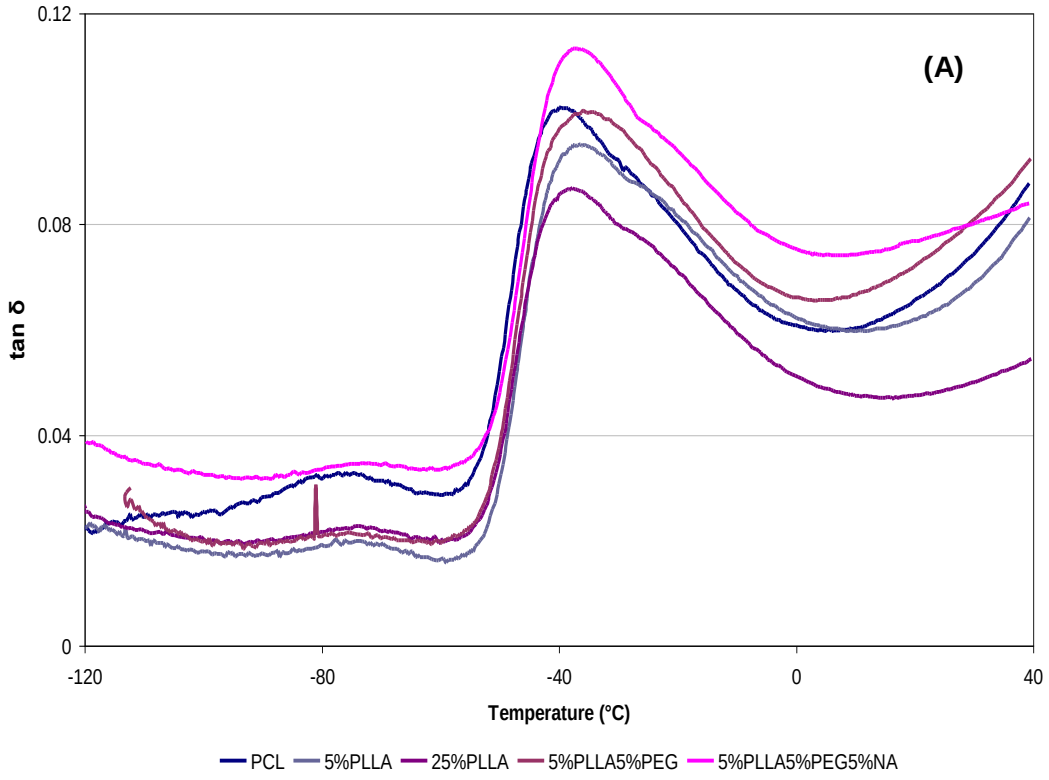
(A)
0.12
0.08
0.04
0
tan δ
-120
-80
-40
0
40
Temperature (°C)
PCL
5%PLLA
25%PLLA
5%PLLA5%PEG
5%PLLA5%PEG5%NA

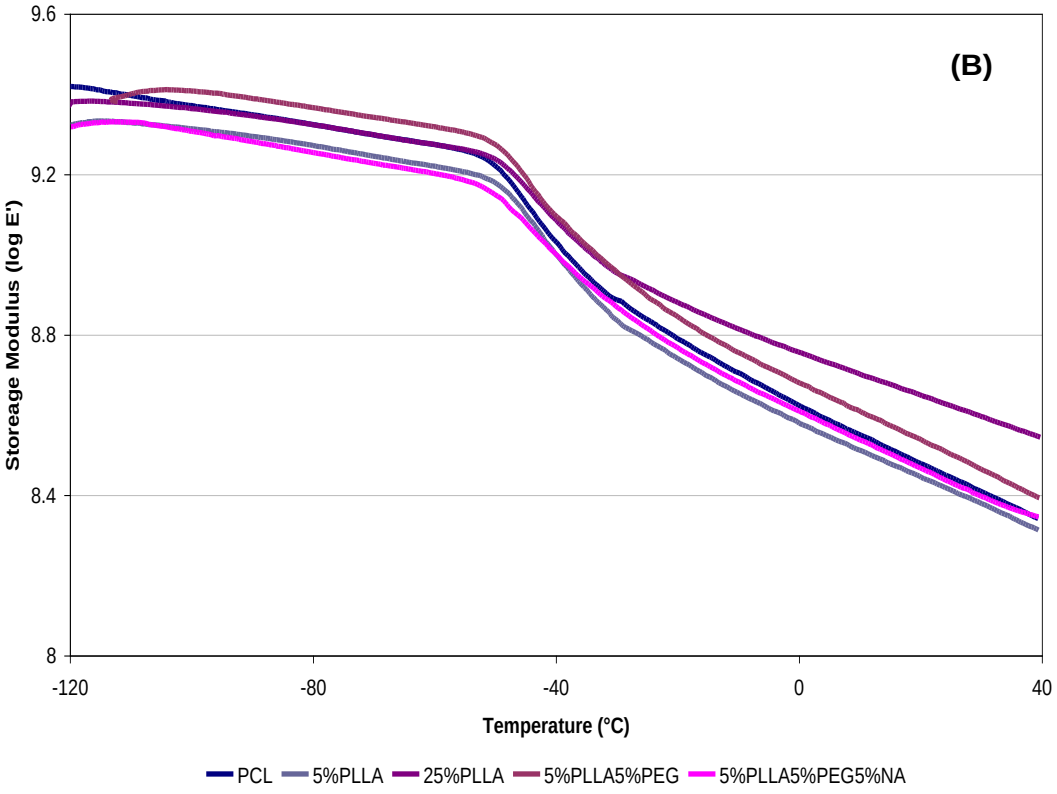
(B)
9.6
9.2
8.8
8.4
8
Storeage Modulus (log E')
-120
-80
-40
0
40
Temperature (°C)
PCL
5%PLLA
25%PLLA
5%PLLA5%PEG
5%PLLA5%PEG5%NA

Figure 2: (A) Tan δ temperature sweeps for PCL-PLLA blends; (B) Storage modulus for PCL-PLLA blends.

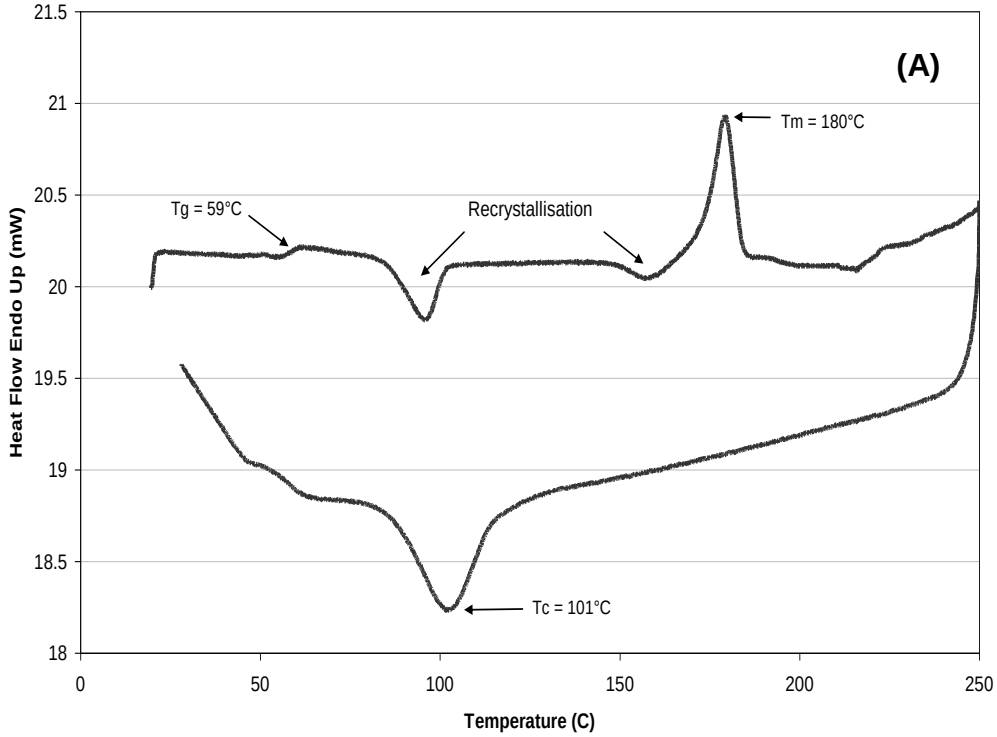

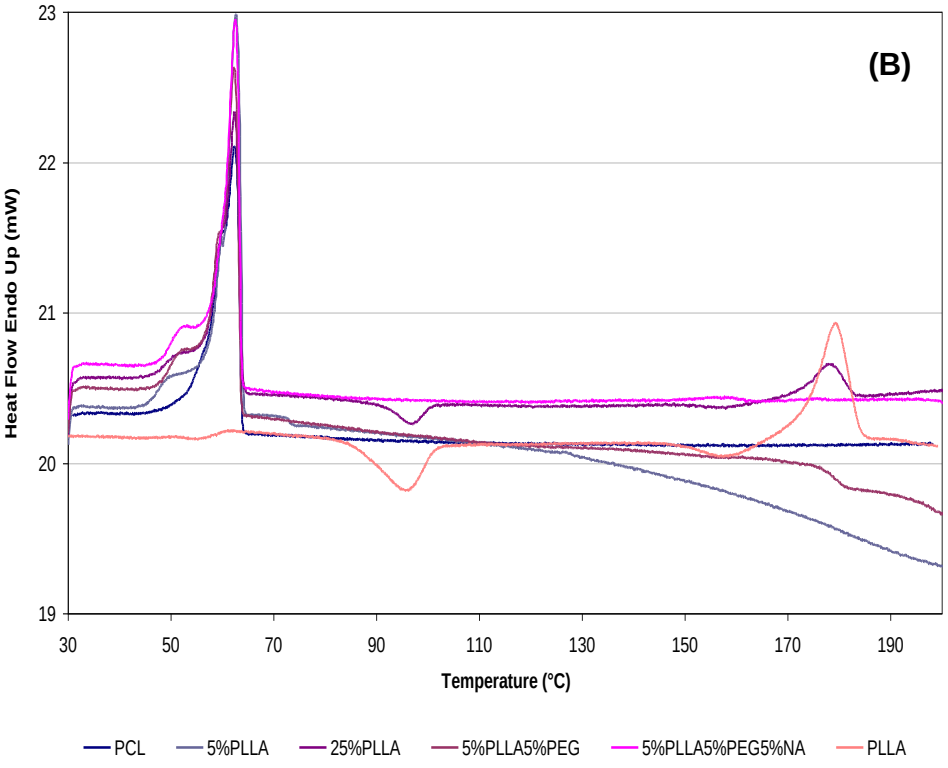

Figure 3: (A) DSC trace of PLLA and (B) Heating scans for PCL-PLLA blends at 2°C/min.

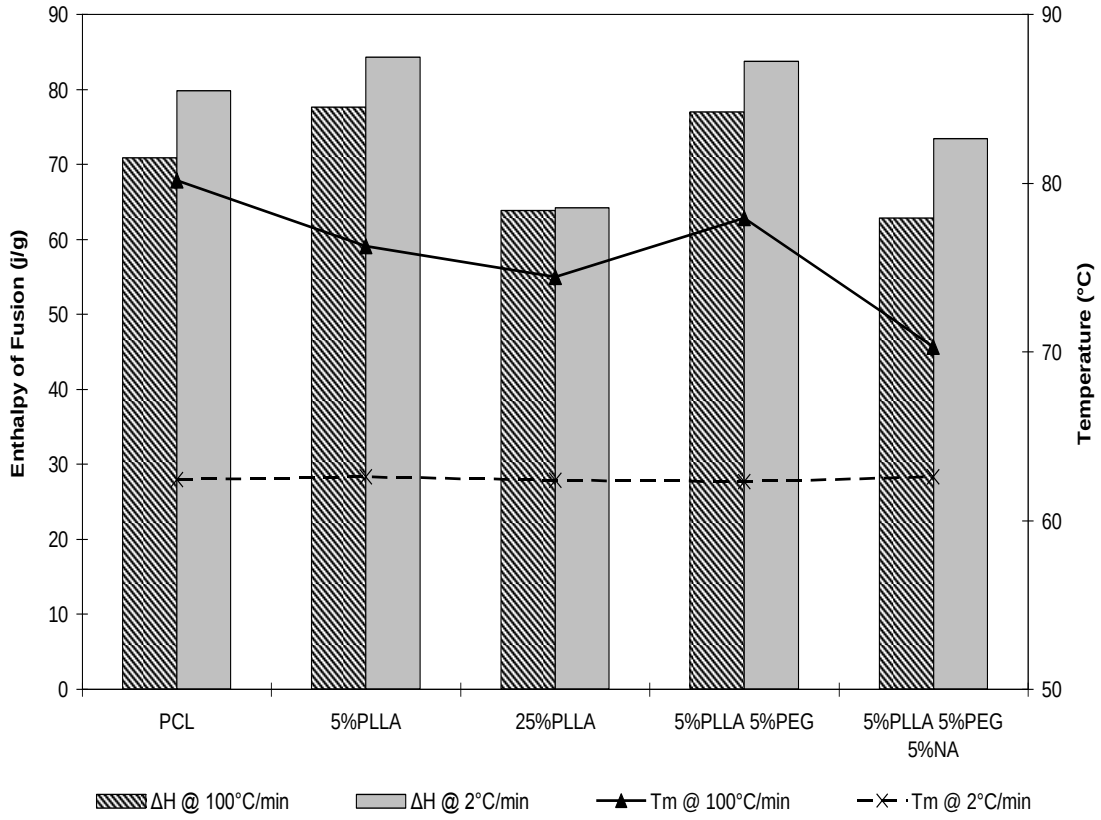

Figure 4: Variation in thermal properties caused by increase DSC scan rate for PCL-PLLA blends.

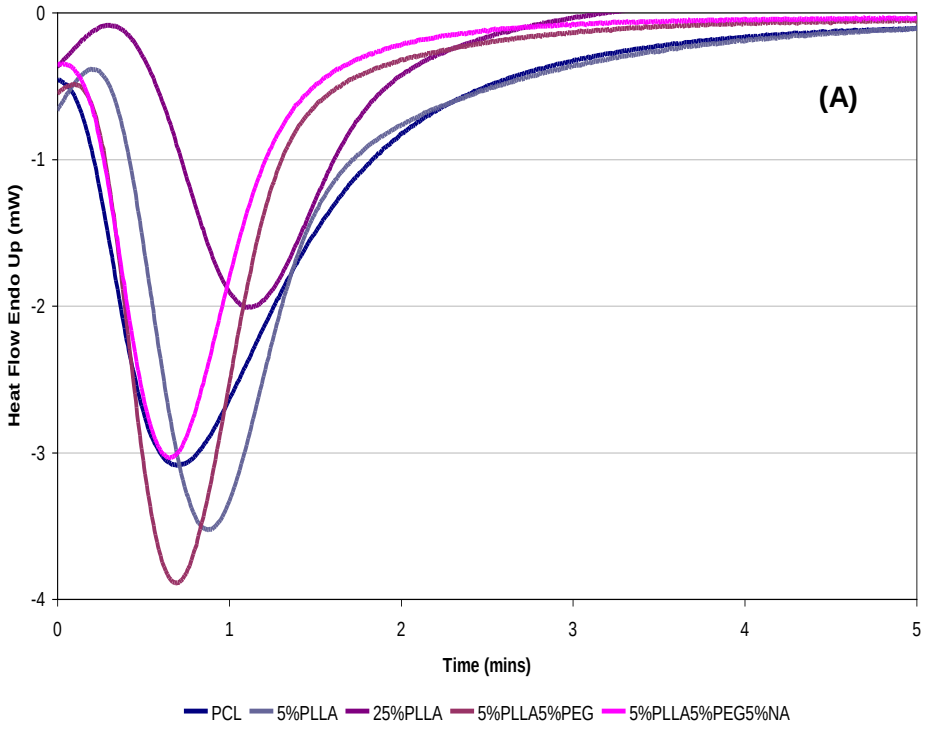
(A)
Heat Flow Endo Up (mW)
0
-1
-2
-3
-4
0
1
2
3
4
5
Time (mins)
PCL
5%PLLA
25%PLLA
5%PLLA5%PEG
5%PLLA5%PEG5%NA

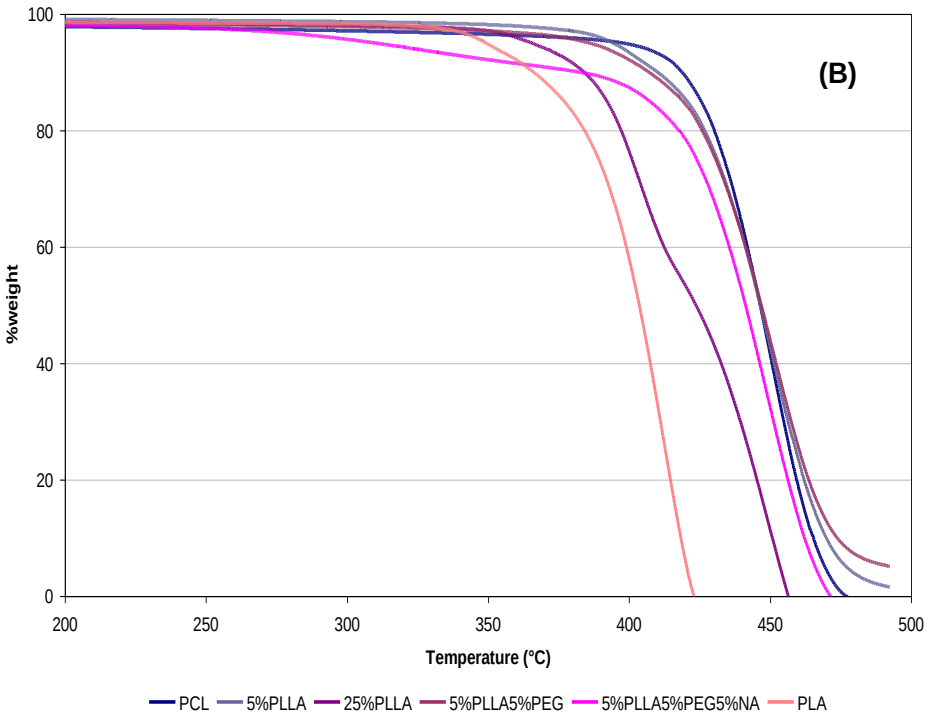
(B)
%weight
100
80
60
40
20
0
200
250
300
350
400
450
500
Temperature (°C)
PCL
5%PLLA
25%PLLA
5%PLLA5%PEG
5%PLLA5%PEG5%NA
PLA

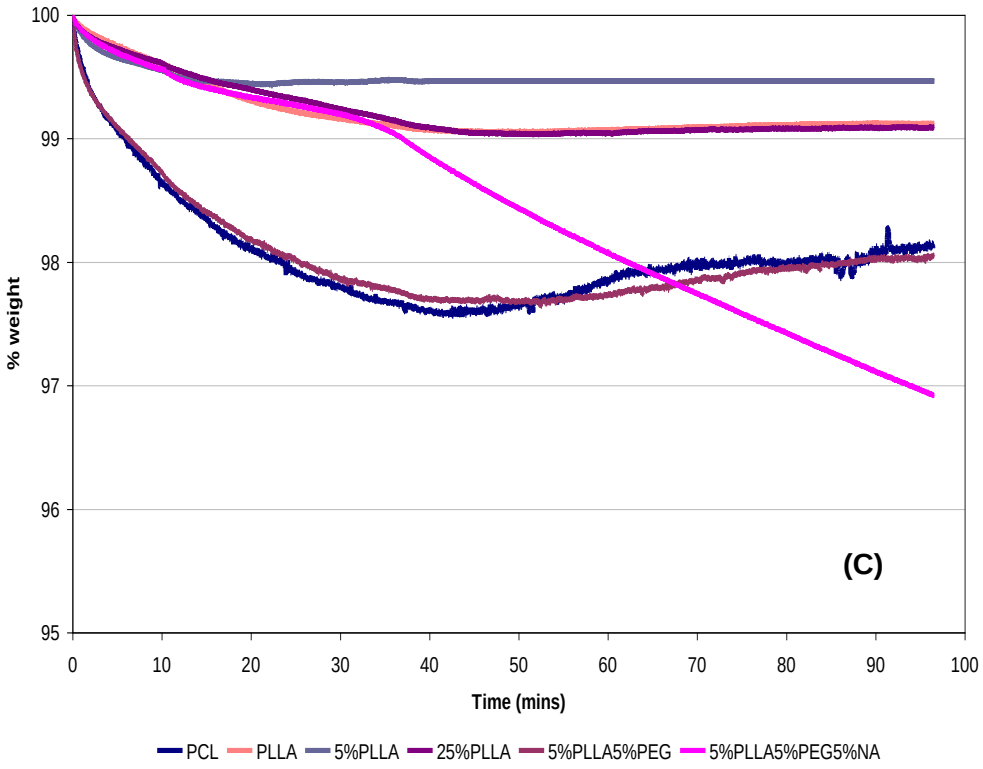

Figure 5: (A) Isothermal scan for PCL-PLLA blends at 38°C; (B) Thermogravimetric analysis of PCL-PLLA blends; (C) Isothermal TGA for PCL-PLLA blends.

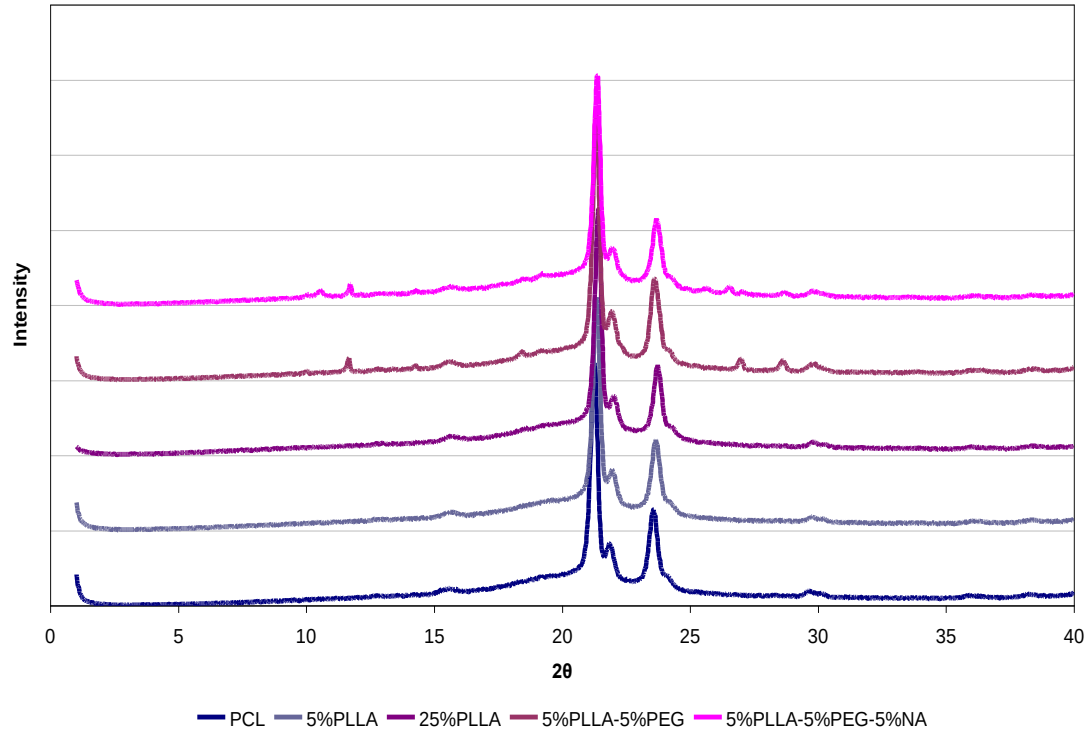

Figure 6: WXRD analysis of PCL-PLLA blends.

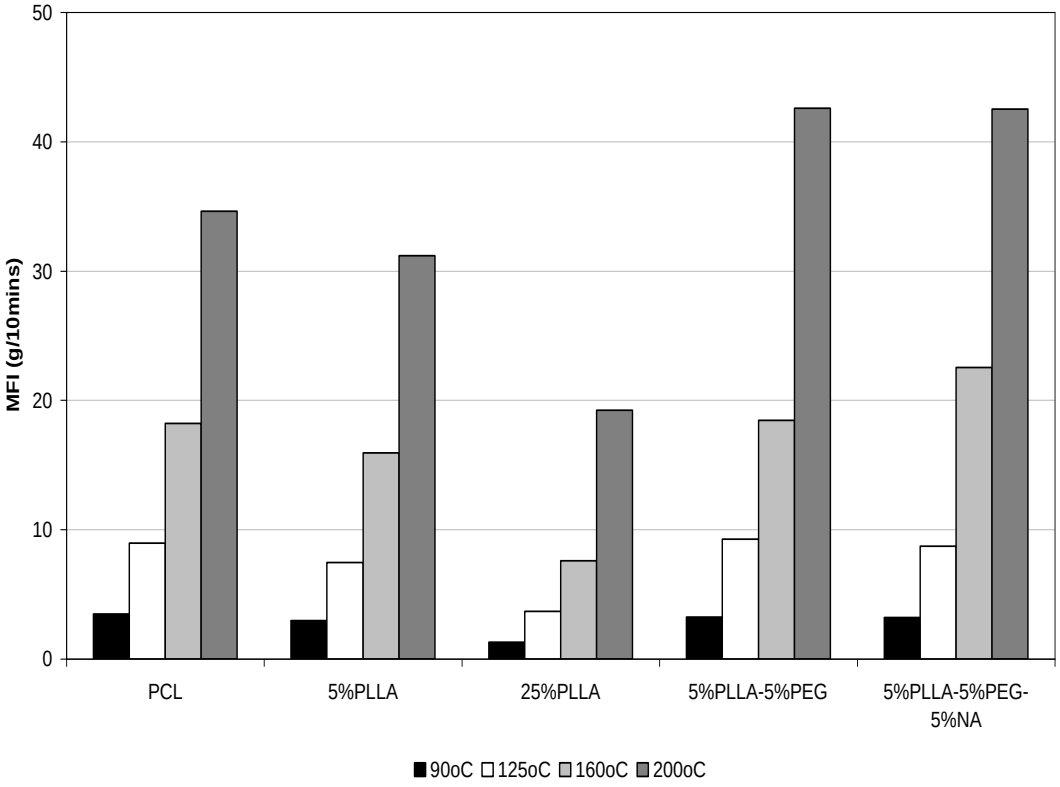

Figure 7: MFI for PCL-PLLA blends at various temperatures.

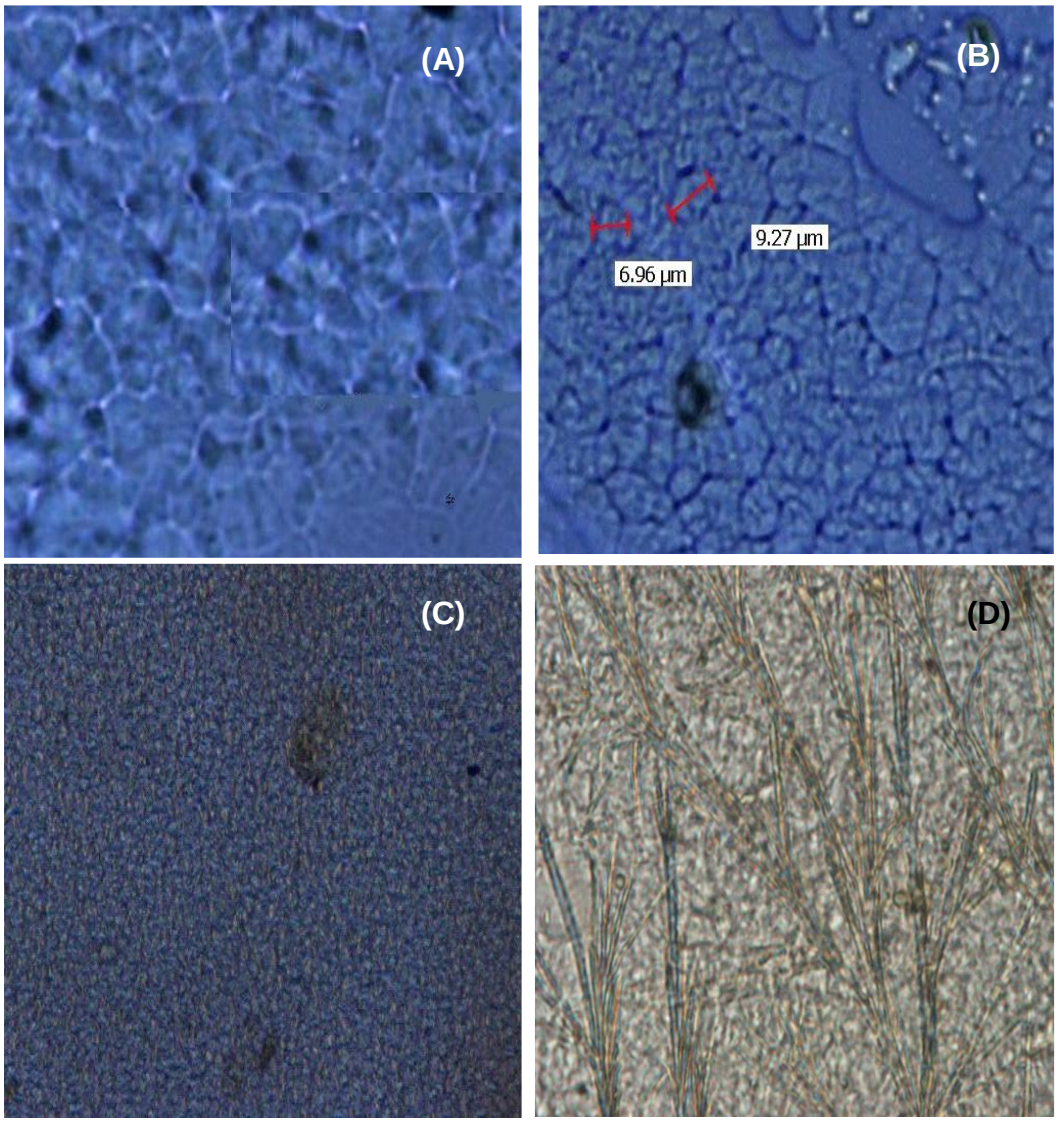

Figure 8: Optical microscopy for (A) 5%PLLA x500; (B) 25%PLLA x500; (C) 5%PLLA-5%PEG x500; (D) 5%PLLA-5%PEG-5%NA x500.

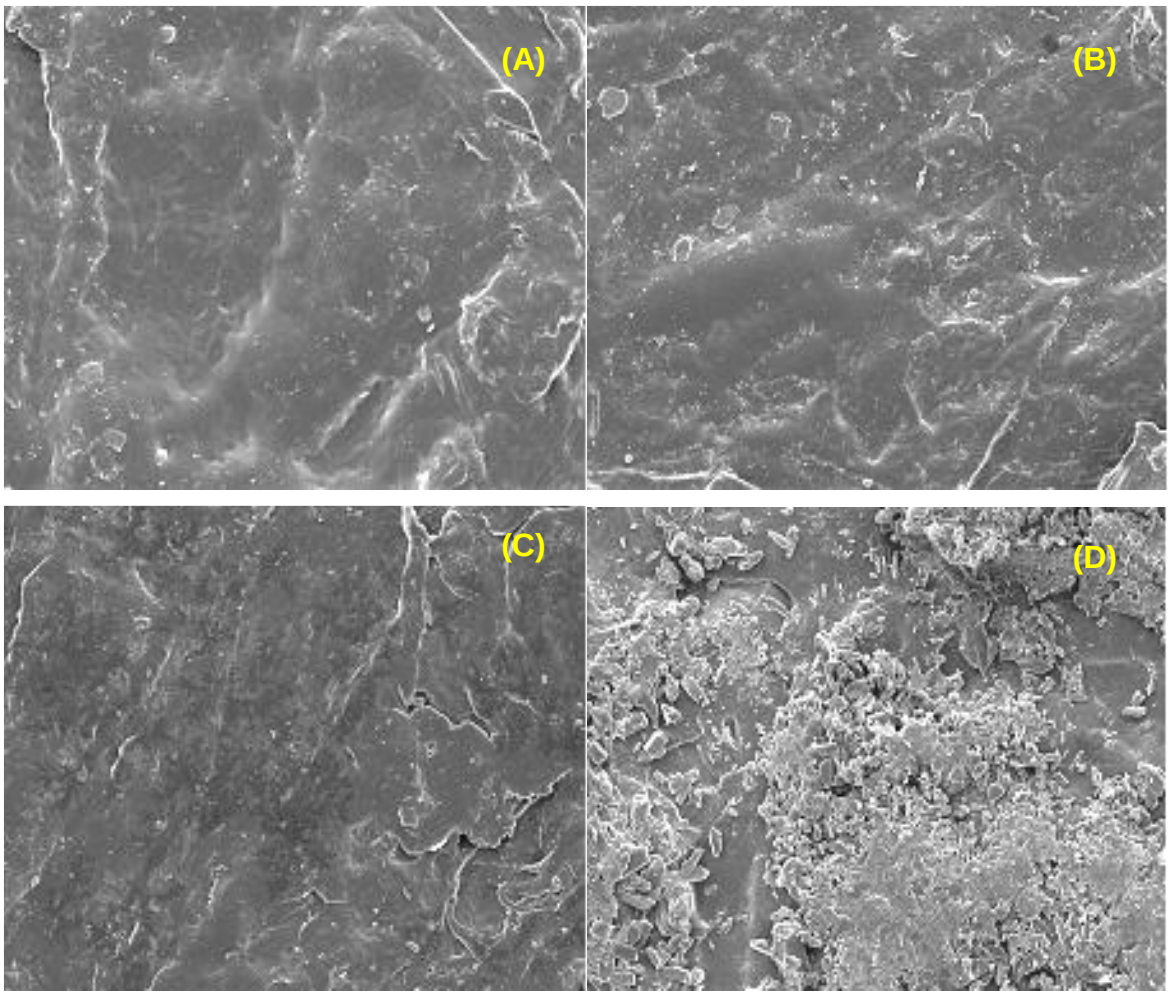

Figure 9: SEM images for (A) 5%PLLA blend x1000; (B) 25%PLLA blend x1000; (C) 5%PLLA-5%PEG x1000; (D) 5%PLLA-5%PEG-5%NA blend x1000.